Late veneer and late accretion to the terrestrial planets

R. Brasser[a,1,*], S. J. Mojzsis[b,c,1,*], S. C. Werner[d,1], S. Matsumura[e,2], S. Ida[a]

[a]*Earth Life Science Institute, Tokyo Institute of Technology, Meguro-ku, Tokyo 152-8550, Japan*
[b]*Department of Geological Sciences, University of Colorado, UCB 399, 2200 Colorado Avenue, Boulder, Colorado 80309-0399, USA*
[c]*Institute for Geological and Geochemical Research, Research Center for Astronomy and Earth Sciences, Hungarian Academy of Sciences, 45 Budaörsi Street, H-1112 Budapest, Hungary*
[d]*The Centre for Earth Evolution and Dynamics, University of Oslo, Sem Saelandsvei 24, 0371 Oslo, Norway*
[e]*School of Science and Engineering, Division of Physics, Fulton Building, University of Dundee, Dundee DD1 4HN, UK*

arXiv:1609.01785v1 [astro-ph.EP] 6 Sep 2016

Abstract

It is generally accepted that silicate-metal ('rocky') planet formation relies on coagulation from a mixture of sub-Mars sized planetary embryos and (smaller) planetesimals that dynamically emerge from the evolving circum-solar disc in the first few million years of our Solar System. Once the planets have, for the most part, assembled after a giant impact phase, they continue to be bombarded by a multitude of planetesimals left over from accretion. Here we place limits on the mass and evolution of these planetesimals based on constraints from the highly siderophile element (HSE) budget of the Moon. Outcomes from a combination of N-body and Monte Carlo simulations of planet formation lead us to four key conclusions about the nature of this early epoch. First, matching the terrestrial to lunar HSE ratio requires either that the late veneer on Earth consisted of a single lunar-size impactor striking the Earth before 4.45 Ga, or that it originated from the impact that created the Moon. An added complication is that analysis of lunar samples indicates the Moon does not preserve convincing evidence for a late veneer like Earth. Second, the expected chondritic veneer component on Mars is 0.06 weight percent. Third, the flux of terrestrial impactors must have been low ($\lesssim 10^{-6}\ M_\oplus\ \mathrm{Myr}^{-1}$) to avoid wholesale melting of Earth's crust after 4.4 Ga, and to simultaneously match the number of observed lunar basins. This conclusion leads to an Hadean eon which is more clement than assumed previously. Last, after the terrestrial planets had fully formed, the mass in remnant planetesimals was $\sim 10^{-3}\ M_\oplus$, lower by at least an order of magnitude than most previous models suggest. Our dynamically and geochemically self-consistent scenario requires that future N-body simulations of rocky planet formation either directly incorporate collisional grinding or rely on pebble accretion.

Keywords: late veneer; lunar bombardment; Hadean Earth; impacts; highly-siderophile elements

1. Introduction

The formation of the terrestrial planets is a long-standing problem that is gradually being resolved. In traditional dynamical models the terrestrial planets grow from a coagulation of planetesimals into protoplanets and subsequently evolve into a giant impact phase, during which the protoplanets collide with each other to lead to the terrestrial planets. Several variations of this scenario exist, of which the *Grand Tack* model is currently popular (Walsh et al., 2011). The Grand Tack relies on early gas-driven migration of Jupiter and Saturn to gravitationally sculpt the inner solid circum-solar disc down to ∼1 AU after which terrestrial planet formation proceeds from solids in an annulus ranging from roughly 0.7 AU to 1 AU. Grand Tack has booked some successes, such as its ability to reproduce the mass-orbit distribution of the terrestrial planets, the compositional gradient, and total mass of the asteroid belt (Walsh et al., 2011). Subsequent evolution of the solar system after terrestrial planet formation, all the way to the present, however, has mostly been studied in separate epochs with disconnected simulations.

Brasser et al. (2016) scrutinised the Grand Tack model in more detail and built a database of simulations that is used here. Since published simulations had rarely been run for much longer than 200 Myr into the evolution of the solar system, we sought to test the model predictions specific to the long-term evolution of the terrestrial system. In this work we calculate the evolution of the terrestrial planets for up to 300 Myr. We aim to obtain the amount of mass accreted by the terrestrial planets after the Moon-forming event and whether this accreted mass is compatible with the highly-siderophile element (HSE) budgets of the inner planets, the early lunar and terrestrial cratering records and the nature of the purported late veneer. We also consider the surface conditions on the Hadean Earth from geochemical data and conclude with the implications of our simulations for future models of terrestrial planet formation.

*Corresponding author
Email addresses: brasser_astro@yahoo.com (R. Brasser), mojzsis@colorado.edu (S. J. Mojzsis)
[1]Collaborative for Research in Origins (CRiO)
[2]Dundee Fellow

2. Constraints from the Moon on the remnant planetesimal mass

The unexpectedly high abundance of HSEs in Earth's upper mantle is a mystery because it is expected that these elements would be effectively sequestered into the core. One popular explanation suggests that Earth accreted a further 0.5-0.8 weight percent (wt%) of its mass after core separation and after the Giant Impact (GI) that formed the Moon (Walker, 2009). The dearth of lunar mantle HSEs indicate that the Moon accreted approximately 0.02-0.035 wt% (Day and Walker, 2015; Kruijer et al., 2015). The ratio of accreted mass between Earth and the Moon is then 1950 ± 650, which is curious because the ratio of the gravitational cross sections of the Earth and Moon is far less ($\sim$20).

There is substantial debate in the literature about a possible late veneer on Mars. Osmium isotopes in martian meteorites indicate that Mars accreted chondritic material after core formation (Brandon et al., 2012), although it is unclear how much material was added to the martian mantle. Walker (2009) suggested that Mars experienced a mass augmentation of $\sim$0.7 wt%, comparable to Earth's. A recent analysis of metal-silicate partitioning for the platinum group elements in martian meteorites, however, combined with theoretical partitioning models used to construct inverse models of Mars' mantle composition, instead show that the concentration of HSEs in the martian mantle can be solely established by metal-silicate equilibration early in the planet's history (Righter et al., 2015). This obviates the need for substantial accretion on Mars during the late veneer epoch. Effective removal of the requirement for much accretion on Mars is important because now the Moon need no longer be regarded as anomalous in the relatively low amount of material it accreted after its formation; only Earth's unusually high HSE abundance demands explanation. This allows us to predict the amount of accretion experienced by Mars when calibrated to the Moon.

The high ratio of the terrestrial and lunar HSE budgets led Bottke et al. (2010) to conclude that the size-frequency distribution of the remaining planetesimals from planet formation had to have been shallow even at large sizes, and the majority of the mass delivered to the Earth should have come from a few large objects comparable to Ceres. The low number of objects leads to a stochastic impact regime for large objects that statistically favours collisions with Earth (Sleep et al., 1989). Hence, the amount of mass accreted on the Moon must be representative of the mass in remnant planetesimals from terrestrial planet formation that are volumetrically smaller than those colliding with Earth.

The probability that the mass of each impactor exceeds m is $P(m) = (m/m_{\rm min})^{-\gamma}$, with $m > m_{\rm min}$. When $\gamma \leq 1$ the total delivered mass is dominated by a single projectile, and the approximate mass delivered to the Earth versus the Moon is $m_{\rm e}/m_{\rm l} = (\sigma_{\rm e}/\sigma_{\rm l})^{1/\gamma}$ (Sleep et al., 1989), where $\sigma_{\rm e,l}$ are the gravitational cross sections of the Earth and Moon, respectively. This ratio can become high when $\gamma \ll 1$. Since $\sigma_{\rm e}/\sigma_{\rm l} \sim 20$, the probability of the Earth being struck by the largest 13 objects is $(19/20)^{13} > 0.5$. The largest verifiable projectile to have struck the Moon created the South Pole-Aitken basin; its diameter was $\sim$170 km (Potter et al., 2012). The collision probability of planetesimals with the Earth is 12% (see below), so there are a total of 100 objects with $D > 170$ km, and thus the expected diameter of the largest projectile (99$^{\rm th}$ percentile) is approximately 1700 km, assuming a main asteroid belt size-frequency distribution ($\gamma \sim 0.7$).

Recently Raymond et al. (2013) showed that a population of planetesimals with a total mass $\sim$0.05 $M_\oplus$ could reproduce the HSE signature in Earth's mantle after the GI over the next few hundred million years. Here we argue that the duration of the time interval that allowed for the mixing of HSEs into the mantle must have been considerably shorter, depending on the exact timing of the Moon-forming event, and should have mostly finished near 4.42 Ga, roughly $\sim$150 Myr after the formation of the proto-Sun at 4.57 Ga. Our arguments for this duration are as follows.

Radiogenic dating of lunar Apollo samples and meteorites indicate that lunar crust formation was well under way by 4.42 Ga (Nemchin et al., 2009), which is the age of the oldest lunar zircon thus far documented. Recent analysis of zircons in martian meteorite NWA 7533 indicates that the earliest crust on Mars formed before 4.43 Ga (Humayun et al., 2013). Taken together these ages suggest that both the Moon and Mars had begun to form a crust some time before 4.42 Ga. In this work, we refer to *late accretion* as those impacts that occurred after continual preservation of the planetary crust. An impact large enough to have destroyed most of the crust and contaminate planetary mantles with HSEs is dubbed a *late veneer*. We shall designate the time interval between the Moon-forming giant impact (GI) near 4.5 Ga and crust formation at 4.42 Ga as the *late veneer epoch* and the time interval after 4.42 Ga as the *late accretion epoch*. Late accretion impacts are inefficient at mixing any HSEs into the mantle and thus the majority of late veneer impacts, which delivered the HSEs, must have occurred before crust formation. The end of the late veneer epoch corresponds closely to the last major differentiation event on the Earth at 4.45 Ga (Allègre et al., 2008), during which the bulk silicate reservoirs were separated when the crust was still molten.

The above arguments can be used to constrain the mass of leftover planetesimals in the inner solar system subsequent to the Moon-forming event, delimiting the rate at which this material is cleared by the terrestrial planets. In principle the total mass of planetesimals decreases with time as $m_{\rm left} = m_{\rm init} f(t)$, where $f(t)$ is the decay function. The amount of mass accreted on the Moon between the time of the GI, assumed to have occurred at 4.5 Ga, and crust formation is

$$m_{\rm init} P_{\rm l} [f(140) - f(60)] = 0.025\,{\rm wt\%} \sim 3 \times 10^{-6}\, M_\oplus, \quad (1)$$

where is $m_{\rm init}$ is the initial mass in planetesimals and $P_{\rm l}$ is the probability of impact of a planetesimal with the Moon. The accretion is measured from 4.5 Ga to 4.42 Ga, the approximate duration of the late veneer epoch in our model. Equation (1) holds regardless of the size-frequency distribution of the remnant planetesimals.

In a collisionless system, the mass in leftover planetesimals follows a stretched exponential decay $m_{\rm left} = m_{\rm init} \exp[-(t/\tau)^{\beta}]$. Brasser et al. (2016) find a stretching parameter $\beta \sim 0.44$, and e-folding time $\tau \sim 12$ Myr. Assuming that this rate of decay holds until the birth of the solar system, substituting 0.5% for the impact probability with the Moon (see below) the mass of remnant planetesimals at the time of the GI is then $m_{\rm left} = 10^{-3}\ M_{\oplus}$.

This mass is at least an order of magnitude lower than the 0.05 $M_{\oplus}$ that Brasser et al. (2016) obtained with the canonical Grand Tack model, or most other terrestrial planet formation simulations. For example, the classical simulations of Matsumura et al. (2016) also have a remnant planetesimal mass of 0.05 $M_{\oplus}$ after 200 Myr. If the estimate of the remaining mass in planetesimals from Brasser et al. (2016) is correct, then after 150 Myr of evolution it is typically 5% of the initial mass. At the time of the Moon-forming impact at 4.5 Ga the planetesimal mass typically is $m_{\rm left} \sim 0.1\ M_{\oplus}$. Then the Moon is expected to be struck by $0.1 \times 0.005 \times [f(140) - f(60)] = 4.2 \times 10^{-5}\ M_{\oplus}$ ~ 0.35 wt%, in contradiction with its HSE budget. In conclusion, the mass in remnant planetesimals *must* have been low ($\lesssim 10^{-3}$ M$_{\oplus}$) at the time the Moon formed.

The above analysis assumes that the mass accreted by the Moon is mostly in the form of small planetesimals so that the accretion can be considered perfect and nearly continuous. These assumptions may not be entirely correct (Bottke et al., 2010; Raymond et al., 2013) and we need to better determine the total accreted mass on each planet. To verify the above claims we ran a series of N-body simulations of the solar system continuing from Brasser et al. (2016), followed by Monte Carlo impact experiments that rely on the impact probabilities from the N-body simulations to determine the total mass of leftover planetesimals, and the relative amount of mass accreted by the Earth, the Moon and Mars for a given size-frequency distribution.

3. N-body simulations of post-formation evolution: Setup and method

We placed the terrestrial planets at their current semi-major axes with their current masses but with much lower initial eccentricities and inclinations that are typical outcomes in Brasser et al. (2016). These will increase later during giant planet migration (Brasser et al., 2013). We placed the gas giants on nearly-circular nearly-coplanar orbits using the configuration of Tsiganis et al. (2005).

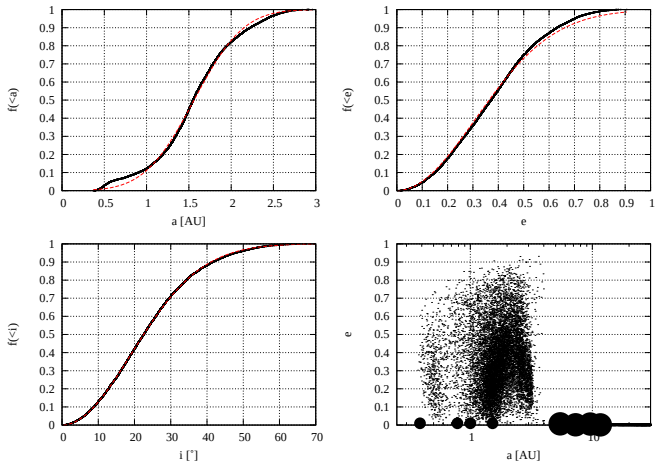


Figure 1: Cumulative distributions (black) and their best fits (red) of the semi-major axis (top, left), eccentricity (top, right), inclination (bottom, left) of the planetesimals that were left after terrestrial planet formation simulations in the framework of the Grand Tack by Brasser et al. (2016). The bottom-right panel shows the distribution of planetesimals in semi-major axis (x) and eccentricity (y), and the positions of the planets.

The initial orbits of the planetesimals were generated from their orbital distribution from the Grand Tack simulations. Even though these include planetesimals from simulations that did not successfully reproduce the terrestrial planets, we concluded that removing these had little influence on the final distribution. Only planetesimals that crossed at least one terrestrial planet but not Jupiter were considered since the latter would quickly eject them. Planetesimals were generated by randomly picking a semi-major axis, eccentricity and inclination from their respective distributions that were fitted with simple functions, and imposing the condition that the maximum perihelion and aphelion distances satisfy $q < 1.5$ AU and $Q < 4.5$ AU (see Supplement). No planetesimal was allowed to be entirely inside of the orbit of Mercury. The other three orbital elements are all angles that were chosen uniformly random from 0 to 360°. With these initial orbits 62% of planetesimals are Earth crossers, 34% cross Venus and just 8% are Mercury crossers. By selection all have their perihelion inside Mars' orbit, and the semi-major axis distribution peaks just beyond Mars' orbit. The fits and initial conditions are shown in Fig. 1.

We impose a size-frequency distribution for the planetesimals so that we have a more realistic amount of mass accreted onto a planet than with equal-mass planetesimals. Following Raymond et al. (2013) our model used a cumulative power-law size distribution with a slope of either 1 or 2 and a planetesimal radius between 250 km and 2000 km or 250 km to 1000 km. A total mass in planetesimals uniformly random from 0.023 $M_{\oplus}$ to 0.077 $M_{\oplus}$, bracketing the typical end values of Brasser et al. (2016), was assumed. The mass of each planetesimal was computed using a density of 3000 kg m^{-3}. We ran 16 simulations for each combination of power law slope and maximum size.

All simulations included the gas giants, terrestrial planets and planetesimals, and were integrated with the symplectic SyMBA

Quantity	Mercury	Venus	Earth	Mars
Mass (wt%)	2.7 ± 4.5	0.8 ± 0.5	0.7 ± 0.5	1.4 ± 2.7
$P_{\rm imp}$ [%]	4.0 ± 0.9	18.0 ± 1.6	12.8 ± 1.8	1.9 ± 0.7
$v_{\rm imp}$ [km s^{-1}]	34.2 ± 13.6	24.3 ± 7.5	21.1 ± 6.2	13.4 ± 5.1

Table 1: The fractional amount of late accreted mass (in wt%), mean impact probability and mean impact speed of projectiles with each planet from the N-body simulations performed here.

package (Duncan et al., 1998) for 150 Myr, covering the epoch from 4.4 Ga to 4.25 Ga, with a time step of 3.65 days. The planetesimals only gravitationally interact with the planets but not with each other. Planetesimals were removed once they were farther than 50 AU from the Sun or when they collided with a planet or ventured closer than 0.1 AU to the Sun. We assume perfect accretion, but ultimately this does not appear to make a large difference (Raymond et al., 2013).

4. Results from N-body simulations

The fraction of remaining planetesimals decreases as a stretched exponential $f = \exp[-(t/\tau)^{\beta}]$ with $\beta = 0.85 \pm 0.07$ and $\beta \log \tau = 1.6 \pm 0.15$. This decay law is similar to a roughly exponential function with e-folding time 100 Myr. After 300 Myr of Solar System evolution (150 Myr from the simulations of Brasser et al. (2016) and a further 150 Myr here) there is still about 1.5% of the total mass left in remnant planetesimals. This result does not account for their collisional evolution.

It appears that Mars is the bottleneck in eliminating this population on long time scales. Encounters with Mars are weak so that the transfer time to Earth-crossing orbits is long. This slow removal of Mars crossers is a property of the Solar System, and is the most likely reason for the initial semi-major axis distribution of the planetesimals peaking near the orbit of Mars.

In Table 1 we list the fractional amount of mass added to each planet, the mean collision probability and mean impact speed of a planetesimal with each planet. The impact probability is computed as the number of planetesimals that collide with a terrestrial planet divided by the total number of planetesimals at the start of the simulation (see Supplement). The reported uncertainties herein are the standard deviations between different simulations. The values computed with this method are consistent with the previous counts within uncertainties; the average probability of colliding with the Moon is 0.53% and the average lunar impact speed is 17 km s^{-1}.

Our results indicate that during the late veneer and late accretion epochs the terrestrial planets all accrete a comparable amount of their total mass. To determine whether the remaining planetesimal mass and clearing rate are physically plausible, their removal through impacts needs to be compared to the lunar cratering record and constraints imposed by geochronology. Better statistics are needed of the nature of the impacts on each planet by taking into account the size-frequency distribution of the projectiles and impact velocities. To address this we turn to a series of Monte Carlo impact experiments, described below.

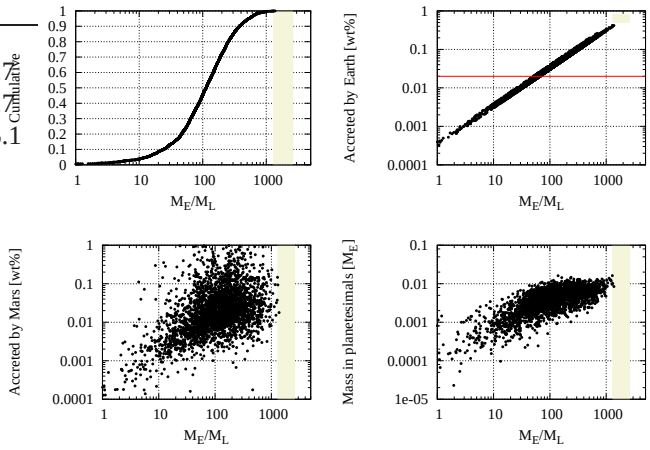


Figure 2: Results of Monte Carlo impact simulations. The *x*-axis is always the ratio of mass accreted by Earth versus that of the Moon. The range in the ratio implied from the HSE element abundance is highlighted in beige, and is taken as 1950 ± 650. Top-left: Cumulative fraction of ratio of accreted mass. Top-right: total mass fraction accreted by the Earth (wt%). The red line is the threshold for wholesale melting of the crust. Bottom-left: total mass fraction accreted by Mars (wt%). Bottom-right: total mass in remnant planetesimals ($M_{\oplus}$).

5. Monte Carlo impact simulations

We calculate the diameter of a random planetesimal between 1 km and 2000 km with a size-frequency distribution that matches the main asteroid belt. It was assumed that each planetesimal has a density of 3000 kg m^{-3} and its mass is added to the total mass. We determine whether the planetesimal will collide with either Earth or Mars using the impact probabilities listed on the second row of Table 1, assuming that these are valid during the late veneer epoch; it is noteworthy that the probability of colliding with the Moon is barely affected by lunar tidal evolution because the Moon's gravitational focusing is negligible. If the planetesimal strikes one of these three bodies, its mass is added to the total mass accreted by the target because we assume perfect accretion for simplicity. We continue to generate planetesimals until the Moon has accreted 0.025 wt%. Our runs are time-independent, so we used them to check accretion during both the late veneer epoch and subsequent late accretion epoch. During the late accretion epoch the accreted mass is halved: applying the same methods and decay law from Section 2 we calculate that the total mass impacting the Moon after the late veneer epoch and until 4.25 Ga is 0.013 wt%.

The results for the late veneer epoch are shown in Fig. 2. The top-left panel displays the cumulative fraction of the ratio of mass accreted by the Earth and the Moon. The beige band indicates the range from HSE data. It is evident that the probability of matching the observed high ratio of accreted mass

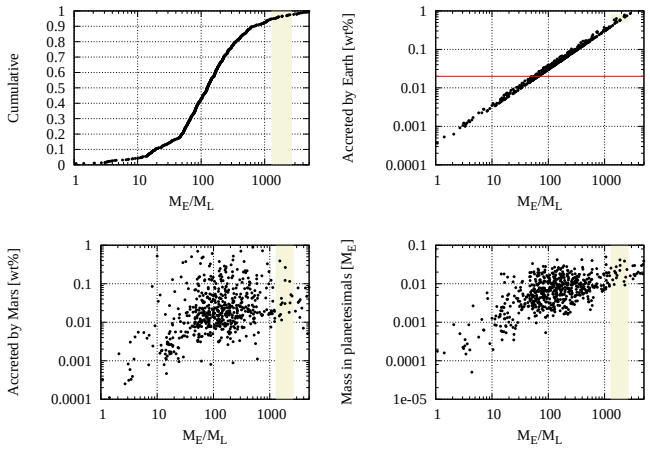


Figure 3: Same as Fig. 2 but in this case the maximum diameter of the planetesimals is increased to 4000 km.

is below 1%, and thus reproducing this high amount of relative accretion between the Earth and the Moon from leftover planetesimals with diameters $D < 2000$ km is unlikely. The top-right panel shows the amount of mass accreted by Earth. The bottom-left panel displays the fractional amount of mass accreted by Mars. This is generally of the same order as the fractional amount accreted by the Earth: the mean mass accreted by Earth is 0.05±0.04 wt% and for Mars is 0.06± 0.03 wt%. Last, the bottom-right panel shows the total mass in remnant planetesimals from terrestrial planet formation. The mean total mass in planetesimals at the time of the Moon-forming impact is typically 0.0046 $M_\oplus$, lower than what was found in Brasser et al. (2016), but still higher than what is predicted by the analysis in Section 2.

The results in Fig. 2 are cause for concern. Our setup rejects the observed HSE ratio between the Earth and Moon during the late veneer epoch at > 99% confidence. Marchi et al. (2014) were unable to reproduce the HSE ratio with a maximum plantesimal diameter of 1000 km. As such, we increased the maximum planetesimal diameter to 4000 km in like manner. The results are displayed in Fig. 3. It is now possible to reproduce the terrestrial to lunar HSE ratio at the 5% level and the average total mass colliding with Earth is 0.11 ± 0.22 wt%, for Mars it is 0.15 ± 0.34 wt% and the total leftover planetesimal mass is 0.01 $M_\oplus$.

We subsequently ran both models for the late accretion epoch, during which the Moon is expected to accrete an additional 0.013 wt%. The results are similar to what is displayed in Fig. 2 but the Earth now only accretes an average of 0.03 ± 0.03 wt% and Mars 0.03 ± 0.02 wt% and the mass in leftover planetesimals is approximately 0.003 $M_\oplus$; these values increase to 0.05 ± 0.13 wt%, 0.03 ± 0.17 wt% and 0.05 $M_\oplus$ when the largest planetesimal's diameter is 4000 km.

Even though increasing the largest planetesimal diameter allows us to reproduce the measured HSE ratio, it is likely that the intensity of the bombardment and the high number of large ($D > 1000$ km) objects striking the Earth violates geochemical and geochronological constraints. Abramov et al. (2013) state that an addition of 0.03 wt% over 100 Myr will cause ∼ 50% of Earth's crust to experience melting, while Marchi et al. (2014) claim that the intensity of their early bombardment causes a cumulative fraction of 100-400% of Earth's crust to be buried by impact melt.

A major episode of post-late veneer wholesale crustal melting is inconsistent with the geochronology and there are multiple lines of evidence that support this claim. First, the last major differentiation event of the Earth's crust occurred near 4.45 Ga (Allègre et al., 2008) (cf. Roth et al. (2013)). This claim is supported by recent measurements of deep-seated chondritic xenon in the mantle that indicate its source has been isolated from the rest of the mantle around 4.45 Ga (Caracausi et al., 2016). Second, there are terrestrial zircons dating back to 4.38 Ga (Valley et al., 2014), which would not have survived such an intense bombardment. Third, Ti-in-zircon thermometry results by Wielicki et al. (2012) conclude that zircon derived from impactites do not represent a dominant source for the Hadean grains thus far documented from Western Australia. Fourth, Carley et al. (2014) show from Ti-in-zircon thermometry analysis that Hadean zircons generally formed in a lower-temperature environment than Icelandic mid-ocean ridge basalt; and finally, the Monte Carlo experiments of Marchi et al. (2014) indicate that the Hadean crust should all be gone, inconsistent with the oldest age of terrestrial zircons, and slightly older zircons from the Moon and Mars (Nemchin et al., 2009; Humayun et al., 2013). Taken together, the geochronology indicates that the amount of impacted mass on the Hadean Earth had to be low, and direct lines of evidence mitigate a late veneer on Earth after ca. 4.45 Ga (Frank et al., 2016).

We are faced with two incompatible constraints: on the one hand we want the accreted mass on the Earth and Mars to be low while at the same time we want the Earth to accrete enough to explain the terrestrial to lunar HSE ratio. One way to solve this dilemma is to assume that the accretion was not as stochastic as displayed in Fig. 2. The most parsimonious way to match these constraints simultaneously is if the event that delivered the HSEs to the Earth's upper mantle after core formation was from a singular late veneer impact unique to Earth, followed by very little accretion afterwards from the background flux of remaining planetesimals. The idea of the late veneer from a small number of big objects is not new (Bottke et al., 2010), but our analysis leads us to conclude it was most likely a single impact, rather than several, and certainly not a multitude. This would also most likely result in a low amount of accretion ($\lesssim$ 0.1 wt%) on Mars after 4.5 Ga.

6. Implications and predictions

6.1. The Late Veneer as a singular event

If the late veneer on the Earth is caused by a single impact, a roughly lunar-sized impactor striking Earth would shatter its

core and cause its HSEs to be suspended in the terrestrial mantle. Conceptually, a singular late veneer event to Earth is not inconsistent with the geochemistry, and is supported by the evolution of tungsten isotopes in the terrestrial mantle. Willbold et al. (2011) state that the pre-veneer terrestrial mantle has an excess of ^{182}W compared to the current mantle of ε^{182}W= 0.15 − 0.2, while the current mantle sits at 0. Willbold et al. (2011) conclude that approximately 0.8 wt% of Earth's mass had to have been added in chondritic proportions to offset this excess ^{182}W; this estimate is compatible with Walker (2009). The chondritic tungsten isotopes from such a 'stray dog' impactor would then subsequently be homogenised in the mantle on a time scale of about 1 Gyr (Maier et al., 2009; Frank et al., 2016); we add that a similar process can be traced by ε^{142}Nd (Roth et al., 2013). During the GI the impactor's core is thought to merge with Earth's through the terrestrial magma ocean(Canup and Asphaug, 2001). In this models of Willbold et al. (2011, 2015) this process preserves the pre-late veneer mantle with ε^{182}W= +0.15. In the late veneer epoch a single lunar-sized object struck the Earth and augmented its mass with chondritic material (ε^{182}W∼ −2) to the pre-late veneer mantle. Convective processes in the 'upper mantle mixed this late veneer material to ultimately homogenise the mantle. By ca. 3300 Ma top-to-bottom homogenisation of the late veneer material is mostly complete in the mantle except for lower mantle domains, which are expected to have preserved a pre-late veneer ε^{182}W signature. Modern-day plate tectonics and mantle convection will do the rest to homogenise the upper mantle in ε^{182}W (Willbold et al., 2015). The Late Veneer mechanism is not universally accepted, however, and alternative interpretations of HSE in the mantle have been presented.

A late veneer consisting of a steady flux of small impactors will not reproduce the HSE ratio because then the terrestrial to lunar mass accretion should be comparable to their gravitational cross sections, which geochemical data show is not the case.

The origin of this 'stray dog' embryo is difficult to trace. Since Jupiter clears about 99.5% of the planetesimals beyond 1 AU in the nominal Grand Tack model, it is likely the embryo originated from closer to the Sun or was pushed inwards by Jupiter and subsequently rattled around the inner solar system until it collided with Earth. Alternatively there were originally more than four terrestrial planets and that the system of multiple planets became unstable in the first 100 Myr. The unstable fifth planet then subsequently collided with the Earth in the form of the late veneer.

Such a late impact may also account for the inclination offset between the lunar orbit and the Earth's spin. A grazing impact near Earth's pole with a lunar-sized object at escape velocity changes Earth's obliquity by approximately

$$\delta\varepsilon = (m/Cm_{\oplus})(Gm_{\oplus}/R_{\oplus}^{3})/\nu^{2} \sim 15^{\circ}, \qquad (2)$$

where C is normalised the moment of inertia and ν is the rotation rate. In the equation above we used a rotation period of 14 h and $C = 0.33$. Such an impact obviates the need for many close encounters between the Moon and remnant planetesimals (Pahlevan and Morbidelli, 2015).

In principle, the Earth's HSE signatures could also be generated from the impactor's core that produced the Moon. Some impactor material formed into the lunar core with most being suspended in the Earth's upper mantle (Newsom and Taylor, 1989; Sleep, 2016) because of Earth's stronger gravity (Kraus et al., 2015). The benefit of this approach is that it does not require a second large impact on Earth. The resulting HSE ratio can then be arbitrarily large or small, and thus reproducing the HSE ratio becomes a matter of the exact nature of the impact. We do note that most Moon-forming impact scenarios yield a molten target Earth that results in merger of the impactor's core with that of the proto-Earth(Canup and Asphaug, 2001). Under these conditions, the HSEs should have been effectively stripped from Earth's mantle and segregated. In this study, however, we cannot rule in favour of either scenario.

6.2. Lunar cratering record

A dynamical model of terrestrial planet formation should be able to quantitatively reproduce the number of known ancient lunar craters, including the basins, over the time span of a few hundred million years. Here we test our Monte Carlo simulations against the lunar basin record and cratering chronology, using the established work of Neukum et al. (2001) and the recent model of Werner et al. (2014).

After the lunar crust began forming near 4.42 Ga (Nemchin et al., 2009), the decrease in the number of planetesimals is either monotonic from at least 4.3 Ga onwards (Werner et al., 2014) or suffered a temporary uptick caused by a possible Late Heavy Bombardment (LHB) that could have coincided with Nectaris basin formation (Bottke et al., 2012). The latter requires a lunar magma ocean solidification time much later than current theoretical estimates (Kamata et al., 2015). Based on stratigraphic relations Wilhelms (1987) lists about 30 pre-Nectarian basins, and 12 basins formed during the Nectarian epoch. In Fig. 4 we plot the cumulative age of 30 lunar basins which are reliably dated using the chronology function of Neukum et al. (2001) (top) and of Werner et al. (2014) (bottom). The ages of South Pole-Aitken and Nectaris basins are 4.22 ± 0.03 and 4.05 ± 0.01 Ga respectively for the former model, and 4.44 ± 0.04 and 4.17 ± 0.02 Ga using the latter model. Thus the late accretion epoch approximately coincides with the range from South Pole-Aitken to Nectaris with the Werner chronology. From our N-body simulations we find that after 4.4 Ga the planetesimal population still decays following a stretched exponential; between 4.4 Ga and 4.2 Ga this decay mimics a regular exponential with e-folding time 100 Myr (see Section 4). This decay rate corresponds reasonably well with that advocated by Neukum et al. (2001) (140 Myr), but is faster than that suggested by Werner et al. (2014) (200 Myr). The main difference between the two applied models is that the basins were formed in periods stretching either over 650 or 900 million years.

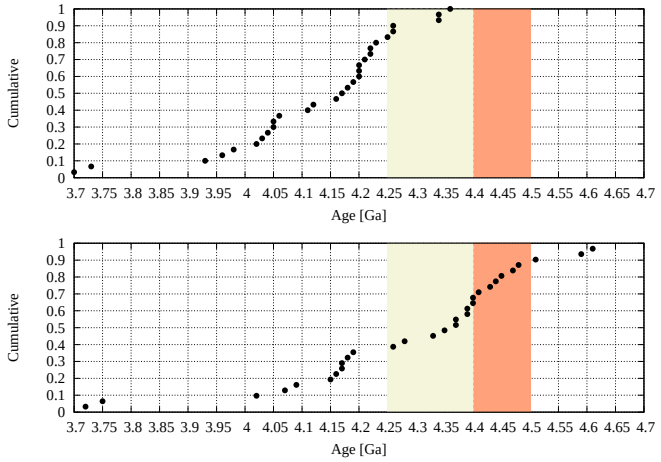


Figure 4: Cumulative lunar basin formation ages for basins with reliable ages. The salmon and beige regions indicate the late veneer and late accretion epochs respectively. Ages calculated using crater statistics (relative sequence) and two different chronology models to determine absolute model ages: Neukum (top) and Werner (bottom). Some of the measurements have limited statistics and thus the derived ages have large error bars (of up to 0.1 Ga).

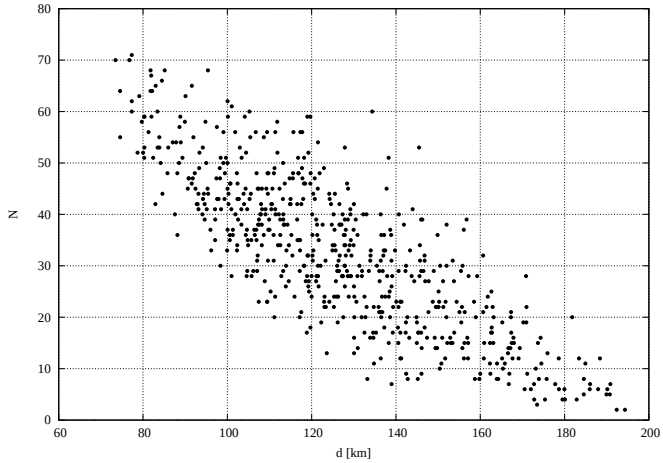


Figure 5: Number of basins produced during the late accretion epoch as a function of the size of the largest planetesimal colliding with the Moon. The more very large basins are produced the smaller is the total number because the total mass accreted onto the Moon is fixed.

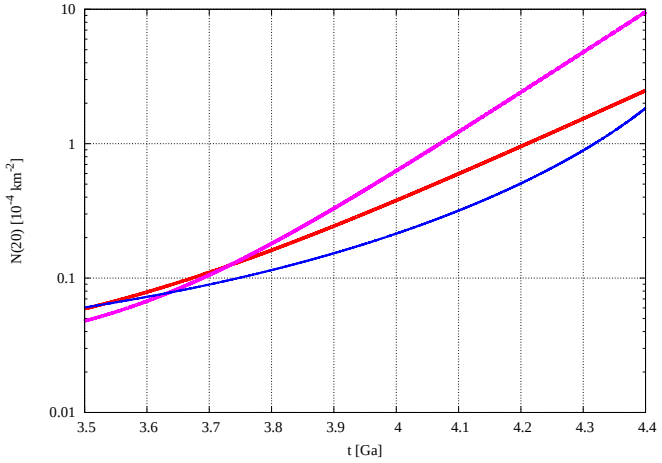


Figure 6: Chronology curves on the Moon, which show the number of 20 kilometre craters per unit area, $N(20)$ with time. We plot the Neukum chronology curve (magenta) (Neukum et al., 2001), Werner chronology curve (red) (Werner et al., 2014) and the chronology curve from the remnant planetesimals (blue).

Basin formation derived from a dynamical model and observed record depends on the assumed projectile-basin diameter relationship and their underlying size-frequency distribution. We follow the detailed analysis of several crater scaling laws for both smaller-sized and larger craters from Minton et al. (2015) and Johnson et al. (2016). For the Moon, we employ a mean impact speed of 17 km s^{-1} and simple-to-complex crater diameter $D_{\rm SC}$ = 15 km (Johnson et al., 2016), and an impact angle of 45°.

In our Monte Carlo impact experiments, we use an impactor size of $D > 22$ km (forming a basin $D_{\rm c,fin} > 300$ km) as threshold. Thus, whenever an object with this diameter, or larger, strikes the Moon we assume that a basin is made and we count the number of such basins. Using the same methodology, we also keep track of the number of small craters we produce with diameter $D_{\rm c,fin} = 20$ km, which we shall use as an independent calibration of the decay function. Thus, in the Monte Carlo simulations, an object with diameter $1 < D < 1.1$ km is considered to have created a 20 km crater.

In Fig. 5 we plot the number of basins created as a function of the diameter of the largest planetesimal that struck the Moon during the late accretion epoch. Note that the Moon is not struck by any object larger than about 200 km in diameter, for which most collisions are accretionary (Raymond et al., 2013). Therefore our earlier assumption of 'perfect' accretion is justified. From Fig. 4 we can interpret the currently observed lunar basin record to be produced either between 4.3 – 3.7 Ga with the Neukum chronology or between 4.4 – 3.7 Ga employing the Werner chronology. Any basins created before 4.4 Ga are most likely erased by crust formation. The number of lunar basins produced during the late accretion epoch is roughly five when using the Neukum chronology, so that the largest impactor should have been very large ($D > 180$ km) to be consistent with the estimated accreted mass. The projectile that produced the SPA basin is thought to have had a diameter of about 170 km (Potter et al., 2012). The Werner chronology produces ten basins during the late accretion epoch, which comports with a $D > 180$ km projectile within error margins. These results suggest that the South Pole-Aitken basin formed some time during or maybe just before the late accretion epoch, in agreement with the age estimates presented earlier.The leftover planetesimals can provide us with 40 basins and the largest impactor does not exceed ~140 km in diameter during the late accretion epoch.

Another test of the model is to determine the temporal cumulative density of craters with a diameter of 20 km per km^2. This quantity, $N(20)$, is calculated as follows for the Moon. Between 4.5 Ga and 4.42 Ga our Monte Carlo simulations pro-

duce on average 13 000 craters with a diameter of 20 km. The crater density as a function of time becomes $N(20) = 1.1 \times 10^{-3}\,\mathrm{km}^{-2} \exp[-((4.56-t)/\tau)^{\beta}]$, where t is in Gyr, $\tau = 0.012$ Gyr and $\beta = 0.44$ (Section 2). The extrapolation to 4.56 Ga is fictitious but is needed to obtain the correct decay rate at 4.42 Ga that matches that of the N-body simulations. The blue curve in Fig. 6 depicts our values of $N(20)$ with age, and contains the steady-state contribution from the asteroid belt. The magenta curve is the Neukum chronology curve and the red curve is the Werner chronology curve, extrapolated from $N(1)$ where we assumed the ratio $N(1)/N(20) = 1000$. Our outcome is below the Werner and Neukum chronology curves, indicating a deficit of craters on the Moon if the remnant planetesimals were the sole source of impactors, and suggesting the need for an increased bombardment rate in the more recent past or a different size-frequency distribution at the small end (Werner, 2014).

6.3. Hadean Earth environment

The lower flux of planetesimals colliding with the Earth than what traditional terrestrial planet formation models predict also has important implications for the environment of the Hadean Earth. Our analysis shows that Earth on average accreted 0.03 wt% between 4.42 Ga and 4.25 Ga. This makes the Hadean Earth a much more clement environment than commonly supposed (Sleep et al., 2001). As discussed previously, analysis of Hadean zirons indicates that impacts were not a major source of heating and resurfacing (Valley et al., 2014; Carley et al., 2014), and oxygen isotopes in Hadean zircons suggest that liquid water existed on Earth's surface before 4.3 Ga (Mojzsis et al., 2001). The recent discovery of potentially biogenic carbon trapped as bona fide graphite inclusions in a 4.1 Ga zircon (Bell et al., 2015) yields further tantalising evidence that Earth could have developed a functioning biosphere before 4.1 Ga. Our results are at odds with Marchi et al. (2014), who argue that between 4.15 Ga to 4.5 Ga, well over 400% of the Hadean Earth's surface is buried by impact-generated melt, which would have also boiled the oceans away (Sleep et al., 1989). We would argue that in future works addressing the Hadean Earth environment, only a low impact flux should be considered.

6.4. Terrestrial planet formation models

Our Monte Carlo simulations indicate that there was generally a low amount of mass in remnant planetesimals at the time of the GI. This requires that either there were never many (large) planetesimals to begin with, or most ground to dust through collisional cascades during the assembly of the terrestrial planets. The role and onset of collisional evolution is so far little explored using N-body simulations, because of inherent difficulties. The initial conditions of many of these simulations are composed of an unperturbed disc of planetary embryos embedded in a swarm of planetesimals (e.g. Matsumura et al. (2016)) and the latter would quickly evolve to dust (Kobayashi and Tanaka, 2010). Our result begs the question whether or not these initial conditions are realistic, because one would expect that the planetesimals are ground away on the same time scale that planetary embryos can form. Clearly further study is needed to determine whether these initial conditions are feasible and what the role of collisions are in growing terrestrial planets.

Pebble accretion, in which planetesimals are rapidly grown to the size of planetary embryos through the accretion of pebbles that drift towards the sun through the circum-solar nebula (Lambrechts and Johansen, 2012), does not require a large planetesimal mass. It is possible to use pebble accretion combined with a very low ($< 10^{-3}\ M_{\oplus}$) total mass in planetesimals to reproduce the terrestrial planet system (Levison et al., 2015). This setup never had a high mass in planetesimals to begin with because almost all of the accreted mass on the planets comes from the pebbles. Even though the results of Levison et al. (2015) look like a promising alternative to the traditional oligarchic growth models, pebble accretion is not without its own set of issues, one of which is that there appear to be insufficient planetesimals to damp the orbits of the terrestrial planets to their current values. Collisional fragmentation from giant impacts may alleviate this problem (Genda et al., 2015), but only if these planetesimals are cleared on a short time scale, and that their combined mass is low enough after the GI to be consistent with our above estimates. Future studies on rocky planet formation that rely on pebble accretion may require the inclusion of collisional fragmentation when two embryos collide.

Our results also indicate that relying on late accretion of planetesimals on the Earth coupled with dynamical simulations to pinpoint the timing of the Moon-forming event (Jacobson et al., 2014) cannot work. First, the required amount of mass accreted by the Earth after the GI requires a remnant mass in planetesimals that far exceeds our estimate from Section 4. Second, we have demonstrated that a rain of planetesimals on the Earth that reproduce the required accreted mass is inconsistent with the geochronology and HSE ratio.

7. Conclusions

Here, we determined amount of mass accreted by the terrestrial planets after the Moon-forming event. We compared the outcomes of N-body simulations of the dynamical evolution of the terrestrial planets and remnant planetesimals with Monte Carlo simulations of impacts on the Earth, Mars and Moon. By combining the outcome of these simulations with the lunar HSE budget, cratering record, geochronology and geochemistry, it is shown that

1. from HSE analysis the total mass in planetesimals at the time of the Moon-forming event had to be $\sim 10^{-3}\ M_{\oplus}$ (Section 2);
2. the expected chondritic contribution to Mars during the late veneer epoch is 0.06 wt% (Section 5);
3. the high terrestrial HSE budget was most likely caused by a singular event unique to Earth (Section 6.1);
4. the remnant planetesimals from terrestrial planet formation may account for most lunar basins, but not necessarily most of the small craters (Section 6.2);

5. the surface conditions of the Hadean Earth were much more clement than commonly thought because of a low-intensity bombardment (Section 6.3);
6. new terrestrial planet formation models will need to take collisional evolution into account and explore alternatives to oligarchic growth such as pebble accretion (Section 6.4).

8. Acknowledgements

We thank Laurie Reisberg for reminding us about osmium isotopes in martian meteorites. Norm Sleep and two anonymous reviewers provided us with valuable feedback that substantially improved the paper. RB is grateful for financial support from the Daiwa Anglo-Japanese Foundation, the Astrobiology Center Project of the National Institutes of Natural Science (AB271017), and JSPS KAKENHI (16K17662). RB and SJM acknowledge the John Templeton Foundation - FfAME Origins program in the support of CRiO. SJM is grateful for support by the NASA Exobiology Program (NNH14ZDA001N-EXO). SCW is supported by the Research Council of Norway (235058/F20 CRATER CLOCK) and through the Centres of Excellence funding scheme, project 223272 (CEED). Numerical simulations were in part carried out on the PC cluster at the Center for Computational Astrophysics, National Astronomical Observatory of Japan.

References

Abramov, O., Kring, D. A., Mojzsis, S. J. 2013. The impact environment of the Hadean Earth. Chemie der Erde / Geochemistry 73, 227-248.

Allègre, C. J., Manhès, G., Göpel, C. 2008. The major differentiation of the Earth at 4.45 Ga. Earth and Planetary Science Letters 267, 386-398.

Bell, E. A., Boehnke, P., Harrison, T. M. & Mao, W. L., 2015. Potentially biogenic carbon preserved in a 4.1 billion-year-old zircon. PNAS 112, 1451814521

Bottke, W. F., Vokrouhlický, D., Minton, D., Nesvorný, D., Morbidelli, A., Brasser, R., Simonson, B., Levison, H. F. 2012. An Archaean heavy bombardment from a destabilized extension of the asteroid belt. Nature 485, 78-81.

Bottke, W. F., Walker, R. J., Day, J. M. D., Nesvorny, D., Elkins-Tanton, L. 2010. Stochastic Late Accretion to Earth, the Moon, and Mars. Science 330, 1527.

Brandon, A. D., Puchtel, I. S., Walker, R. J., Day, J. M. D., Irving, A. J., Taylor, L. A. 2012. Evolution of the martian mantle inferred from the ^{187}Re- ^{187}Os isotope and highly siderophile element abundance systematics of shergottite meteorites. Geochimica et Cosmochimica Acta 76, 206-235.

Brasser, R., Walsh, K. J., Nesvorný, D. 2013. Constraining the primordial orbits of the terrestrial planets. Monthly Notices of the Royal Astronomical Society 433, 3417-3427.

Brasser, R., Matsumura, S., Ida, S., Mojzsis, S. J., Werner, S. C. 2016. Analysis of Terrestrial Planet Formation by the Grand Tack Model: System Architecture and Tack Location. The Astrophysical Journal 821, 75.

Canup, R. M., Asphaug, E. 2001. Origin of the Moon in a giant impact near the end of the Earth's formation. Nature 412, 708-712.

Caracausi, A., Avice, G., Burnard, P. G., Füri, E., Marty, B. 2016 Chondritic xenon in the Earths mantle. Nature 533, 82-85.

Carley, T. L., Miller, C. F., Wooden, J. L., Padilla, A. J., Schmitt, A. K., Economos, R. C., Bindeman, I. N., Jordan, B. T. 2014. Iceland is not a magmatic analog for the Hadean: Evidence from the zircon record. Earth and Planetary Science Letters 405, 85-97.

Day, J. M. D., Pearson, D. G., Taylor, L. A. 2007. Highly Siderophile Element Constraints on Accretion and Differentiation of the Earth-Moon System. Science 315, 217.

Day, J. M. D., Walker, R. J. 2015. Highly siderophile element depletion in the Moon. Earth and Planetary Science Letters 423, 114-124.

Duncan, M. J., Levison, H. F., Lee, M. H. 1998. A Multiple Time Step Symplectic Algorithm for Integrating Close Encounters. The Astronomical Journal 116, 2067-2077.

Frank, E. A., Maier, W. D., Mojzsis, S. J. 2016. Highly siderophile element abundances in Eoarchean komatiite and basalt protoliths. Contributions to Mineralogy and Petrology 171, 29-44.

Genda, H., Kobayashi, H., Kokubo, E. 2015. Warm Debris Disks Produced by Giant Impacts during Terrestrial Planet Formation. The Astrophysical Journal 810, 136.

Humayun, M., and 10 colleagues 2013. Origin and age of the earliest Martian crust from meteorite NWA 7533. Nature 503, 513-516.

Jacobson, S. A., Morbidelli, A., Raymond, S. N., O'Brien, D. P., Walsh, K. J., Rubie, D. C. 2014. Highly siderophile elements in Earth's mantle as a clock for the Moon-forming impact. Nature 508, 84-87.

Johnson, B. C., Collins, G. S., Minton, D. A., Bowling, T. J., Simonson, B. M., Zuber, M. T. 2016. Spherule layers, crater scaling laws, and the population of ancient terrestrial impactors. Icarus 271, 350-359.

Kamata, S., and 13 colleagues 2015. The relative timing of Lunar Magma Ocean solidification and the Late Heavy Bombardment inferred from highly degraded impact basin structures. Icarus 250, 492-503.

Kobayashi, H., Tanaka, H. 2010. Fragmentation model dependence of collision cascades. Icarus 206, 735-746.

Kraus, R. G., Root, S., Lemke, R. W., Stewart, S. T., Jacobsen S. B., & Mattsson, T. R. 2015 Impact vaporization of planetesimal cores in the late stages of planet formation. Nature Geoscience 8, 269-272.

Kruijer, T. S., Kleine, T., Fischer-Gödde, M. & Sprung, P. 2015. Lunar tungsten isotopic evidence for the late veneer. Nature 520, 534-537

Lambrechts, M., Johansen, A. 2012. Rapid growth of gas-giant cores by pebble accretion. Astronomy and Astrophysics 544, A32.

Levison, H. F., Duncan, M. J. 1994. The long-term dynamical behavior of short-period comets. Icarus 108, 18-36.

Levison, H. F., Kretke, K. A., Walsh, K. J., Bottke, W. F. 2015. Growing the terrestrial planets from the gradual accumulation of sub-meter sized objects. Proceedings of the National Academy of Science 112, 14180-14185.

Maier, W. D., Barnes, S. J., Campbell, I. H., et al. 2009. Progressive mixing of meteoritic veneer into the early Earth's deep mantle. Nature 460, 620-623

Marchi, S., Bottke, W. F., Elkins-Tanton, L. T., Bierhaus, M., Wuennemann, K., Morbidelli, A., Kring, D. A. 2014. Widespread mixing and burial of Earth's Hadean crust by asteroid impacts. Nature 511, 578-582.

Matsumura, S., Brasser, R., Ida, S. 2016. Effects of Dynamical Evolution of Giant Planets on the Delivery of Atmophile Elements during Terrestrial Planet Formation. The Astrophysical Journal 818, 15.

Minton, D. A., Richardson, J. E., Fassett, C. I. 2015. Re-examining the main asteroid belt as the primary source of ancient lunar craters. Icarus 247, 172-190.

Mojzsis, S. J., Harrison, T. M., Pidgeon, R. T. 2001. Oxygen-isotope evidence from ancient zircons for liquid water at the Earth's surface 4,300Myr ago. Nature 409, 178-181.

Nemchin, A., Timms, N., Pidgeon, R., Geisler, T., Reddy, S., Meyer, C. 2009. Timing of crystallization of the lunar magma ocean constrained by the oldest zircon. Nature Geoscience 2, 133-136.

Neukum, G., Ivanov, B. A., Hartmann, W. K. 2001. Cratering Records in the Inner Solar System in Relation to the Lunar Reference System. Space Science Reviews 96, 55-86.

Newsom, H. E., Taylor, S. R. 1989. Geochemical implications of the formation of the Moon by a single giant impact. Nature 338, 360.

Pahlevan, K., Morbidelli, A. 2015. Collisionless encounters and the origin of the lunar inclination. Nature 527, 492-494.

Potter, R. W. K., Collins, G. S., Kiefer, W. S., McGovern, P. J., Kring, D. A. 2012. Constraining the size of the South Pole-Aitken basin impact. Icarus 220, 730-743.

Raymond, S. N., Schlichting, H. E., Hersant, F., Selsis, F. 2013. Dynamical and collisional constraints on a stochastic late veneer on the terrestrial planets. Icarus 226, 671-681.

Righter, K., Danielson, L. R., Pando, K. M., Williams, J., Humayun, M., Hervig, R. L., Sharp, T. G. 2015. Highly siderophile element (HSE) abundances in the mantle of Mars are due to core formation at high pressure and temperature. Meteoritics and Planetary Science 50, 604-631.

Roth, A. S. G., Bourdon, B., Mojzsis, S. J., Touboul, M., Sprung, P., Gui-

treau, M., Blichert-Toft, J. 2013. Inherited ^{142}Nd anomalies in Eoarchean protoliths. Earth and Planetary Science Letters 361, 50-57.
Sleep, N. H., Zahnle, K. J., Kasting, J. F., Morowitz, H. J. 1989. Annihilation of ecosystems by large asteroid impacts on the early earth. Nature 342, 139-142.
Sleep, N. H., Zahnle, K., Neuhoff, P. S. 2001. Inaugural Article: Initiation of clement surface conditions on the earliest Earth. Proceedings of the National Academy of Science 98, 3666-3672.
Sleep, N. H. 2016. Asteroid bombardment and the core of Theia as possible sources for the Earth's late veneer component. Geochemistry, Geophysics, Geosystems 17, xx-yy
Tsiganis, K., Gomes, R., Morbidelli, A., Levison, H. F. 2005. Origin of the orbital architecture of the giant planets of the Solar System. Nature 435, 459-461.
Valley, J. W., et al. 2014. Hadean age for a post-magma-ocean zircon confirmed by atom-probe tomography. Nature Geoscience 7, 219-223
Walker, R. J. 2009. Highly siderophile elements in the Earth, Moon and Mars: Update and implications for planetary accretion and differentiation. Chemie der Erde / Geochemistry 69, 101-125.
Walsh, K. J., Morbidelli, A., Raymond, S. N., O'Brien, D. P., Mandell, A. M. 2011. A low mass for Mars from Jupiter's early gas-driven migration. Nature 475, 206-209.
Werner, S. C. 2014. Moon, Mars, Mercury: Basin formation ages and implications for the maximum surface age and the migration of gaseous planets. Earth and Planetary Science Letters 400, 54-65.
Werner, S. C., Ody, A., Poulet, F. 2014. The Source Crater of Martian Shergottite Meteorites. Science 343, 1343-1346.
Wielicki, M. M., Harrison, T. M., Schmitt, A. K. 2012. Geochemical signatures and magmatic stability of terrestrial impact produced zircon. Earth and Planetary Science Letters 321, 20-31.
Willbold, M., Elliott, T., Moorbath, S. 2011. The tungsten isotopic composition of the Earth's mantle before the terminal bombardment. Nature 477, 195-198.
Willbold, M., Mojzsis, S. J., Chen, H.-W., Elliott, T. 2015. Tungsten isotope composition of the Acasta Gneiss Complex. Earth and Planetary Science Letters 419, 168-177.
Wilhelms, D. E. 1987. The Geologic History of the Moon. USGS Professional Paper 1348, 1-337.